Vol. 495: 193–204, 2014
doi: 10.3354/meps10571

MARINE ECOLOGY PROGRESS SERIES
Mar Ecol Prog Ser

Published January 9

Particle size, flow speed, and body size interactions determine feeding rates of a solitary ascidian, *Styela plicata*: a flume experiment

Andrew N. Sumerel[1,3], Christopher M. Finelli[1,2,*]

[1]Center for Marine Science, and [2]Department of Biology and Marine Biology, University of North Carolina Wilmington, 601 South College Rd., Wilmington, North Carolina 28403, USA

[3]*Present address:* Cape Fear Community College, 411 North Front St., Wilmington, North Carolina 28401, USA

ABSTRACT: Benthic suspension feeders are a primary conduit for the transfer of carbon from the water column to the benthos. As such, factors that influence their feeding require mechanistic study and quantification. In this flume experiment, the clearance rate of the solitary ascidian *Styela plicata* varied as a function of flow speed, body size, and particle diameter. At all flow speeds and body sizes tested, clearance rates increased directly with particle diameter to ~10 µm. As particle diameter increased further to ~32 µm, clearance remained constant or declined depending on flow speed. At 3 and 22 cm s^{-1}, clearance remained constant with particle diameter >10 µm. At 14 cm s^{-1}, clearance sharply declined as particle diameter increased above 10 µm. In general, clearance rates increased with body size across all particle diameters. However, allometric exponents relating clearance rate to body size, which ranged from 0.28 to 0.62, were lower than expected (~0.67) due to the confounding effects of water flow, to which clearance rate responded in a non-linear fashion. We fit our measurements to a 3-dimensional surface that relates clearance rate, body size, and flow speed. These surface fits show that clearance of small particles (<10 µm diameter) was maximal at intermediate flow speeds (~12 cm s^{-1}) and decreased at both faster and slower flow speeds. This 'unimodal' response is consistent with predictions of suspension-feeding theory. In contrast, clearance of large particles (>10 µm diameter) decreased steadily as flow speed increased from 3 to 22 cm s^{-1}.

KEY WORDS: Suspension feeding · Clearance rate · Flow · Allometry · Benthic–Pelagic coupling · *Styela plicata* · Ascidian

INTRODUCTION AND THEORETICAL DEVELOPMENT

Benthic suspension feeders (BSF) can exert considerable influence over water column processes, especially in shallow bays and where they exist in dense assemblages (Cloern 1982, Officer et al. 1982, Petersen & Riisgård 1992). Because of their ecological importance, factors that influence BSF feeding rates have been the focus of empirical and theoretical study for many decades (Jorgensen 1966, Shimeta & Jumars 1991, Wildish & Kristmanson 1997). Notably, water flow can act as a master variable to influence feeding rates of both passive and active suspension feeders due to its interaction with the organism and its influence on particle flux. *Styela plicata* is a sessile, active suspension feeder that is an abundant and conspicuous member of subtidal fouling communities worldwide. These organisms generate a current that draws particle-laden water from the water column into the inhalant siphon, which is surrounded by tentacles that serve to reject some larger particles. Water passes through the siphon into the pharynx, where it passes through a perforated and ciliated

*Corresponding author: finellic@uncw.edu

branchial basket that produces the feeding current. Particles passing through the branchial basket are retained on a mucus net that is then passed to the esophagus to be digested (Petersen 2007). While larger particles can be rejected by the tentacles, particles entering the pharynx are trapped with high efficiency, often approaching 100% under idealized conditions (Randløv & Riisgård 1979). Some variation in retention efficiency is noted depending on particle size and character (e.g. Fiala-Médioni 1978, Klumpp 1984), with average retention rates of 70 to 85% for particles in the 1 to 50 µm range (e.g. Fiala-Médioni 1978, Randløv & Riisgård 1979, Klumpp 1984).

Earlier studies of ascidian feeding have focused primarily on defining the scope and energetics of ascidian feeding (reviewed in Petersen 2007). Importantly, these studies have been conducted under idealized environmental conditions of small test chamber volume, minimal water flow, and restricted particle size. These conditions are important for establishing maximal feeding rates and particle retention efficiency, but they are less relevant to the field situation in which flowing water acts on both the tunicate body and the flux of food particles. Some recent evidence suggests that juvenile (e.g. smaller) specimens may be at a disadvantage due to greater resistance to flow through narrow siphons, highlighting the importance of siphon morphology in constraining the feeding current (Sherrard & LaBarbera 2005). In contrast, the interaction of ambient flow and morphology may also play a role in enhancing feeding. For example, Young & Braithwaite (1980) and Knott et al. (2004) both suggested that orientation of the tunicate body so that the inhalant siphon was directed into flow passively enhanced feeding by increasing the pressure gradient between inhalant and exhalant openings. These final examples highlight the interaction of ascidian feeding with the external environment and water flow in particular. Here we present the results of a comprehensive flume study of clearance rates of *Styela plicata* as a function of body size, flow speed, and particle size.

We initiated our study by considering the change in clearance rates with body size. 'Body size' has variable meaning in the suspension-feeding literature and is used to describe one of several related terms including body mass (e.g wet mass, dry mass, or ash-free dry mass) and body area projected normal to flow. As body size increases, clearance rate is predicted to increase as described by the allometric relationship such that:

$$CR = s_c S^b \quad (1)$$

where CR is the clearance rate, s_c is an empirical constant, S is body size, and b is a constant (Randløv & Riisgård 1979). (All constants and variables defined in Box 1.) The 'two-thirds' rule (i.e. $b = 0.667$) is the generally accepted comparison for the relationship between clearance rate and body mass (Randløv & Riisgård 1979, Klumpp 1984) and is determined from dimensional scaling of squared dimensions of surface area responsible for filtration (branchial surface) and cubed dimensions of body volume (Klumpp 1984, Schmidt-Nielsen 1997).

In addition to body size, clearance rates of BSF may be influenced by water flow. The flow-dependent clearance rates of BSF are often described as being unimodal, with clearance rate increasing with flow speed to a maximum, and then declining with further increases in flow (e.g. Wildish & Kristmanson 1997). For active suspension feeders in flows slower than the optimum, clearance rate is directly proportional to flow speed due to increasing particle flux, but does not approach zero in still water because these organisms create their own feeding currents. At flow speeds higher than the optimum, CR is predicted to be suppressed due to a variety of causes including particle overloading (Wildish et al. 1992), the development of adverse pressure gradients between inhalant and exhalant siphons (Wildish et al. 1992, Wildish & Saulnier 1993) and changes in body posture due to drag (e.g. Sponaugle & LaBarbera 1991, Finelli et al. 2002).

There is no *a priori* reason for choosing a particular mathematical description of this feeding response to flow. Therefore, for simplicity, we chose to describe the relationship as the symmetrical Gaussian distribution such that clearance rate is a smooth, continuous function of flow speed:

$$CR = CR_0 e^{-\frac{1}{2}\left(\frac{U-U_p}{w}\right)^2} \quad (2)$$

where CR_0 is the clearance rate in still water, U is flow speed, U_p is the flow speed at which maximum (peak) filtration occurs, and w describes the width of the 'bell' curve. Multiplying the right-hand terms of Eqs. (1 & 2), yields a description of clearance rate that is a function of both body size and flow speed

$$CR = cS^b e^{-\frac{1}{2}\left(\frac{U-U_p}{w}\right)^2} \quad (3)$$

where $c = s_c\ CR_0$ (Fig. 1).

Finally, as noted above, the character of suspended particles (size, shape, density, composition) can influence particle retention, either by the mechanics of filtration or through biological sorting. Natural seston

Box 1. List of constants and variables

b – Allometric exponent relating clearance rate to body size (unitless)
b_s – Power-law exponent relating ash-free dry mass to projected body area in still water (unitless)
c – Empirical constant equivalent to body-size-dependent clearance rate in still water (units dependent on body size category)
C_{B0} – Initial concentration of suspended particles during a feeding trial (µl l^{-1})
C_{Bt} – Concentration of suspended particles at time t during a feeding trial (µl l^{-1})
C_{C0} – Initial concentration of suspended particles during a control trial (µl l^{-1})
C_{Ct} – Concentration of suspended particles at time t during a control trial (µl l^{-1})
CR – Clearance rate (l h^{-1})
CR_L – Large-particle clearance rate (l h^{-1})
CR_0 – Clearance rate in still water (l h^{-1})
CR_S – Small-particle clearance rate (l h^{-1})
CR_T – Total clearance rate across the entire particle size range (l h^{-1})
m – Slope of linear regression relating projected area in flow to projected area in still water
S – Body size (units dependent on body size category)
s_c – Empirical scaling constant relating clearance rate to body size
s_s – Empirical scaling constant relating ash-free dry mass to projected body area in still water
S_f – Frontal body area of an ascidian projected normal to fluid flow direction (cm^2)
S_M – Body mass as ash-free dry mass (g)
S_0 – Frontal body area of an ascidian in still water (cm^2)
t – Time (h)
U – Mainstream flow speed (cm s^{-1})
U_p – Flow speed where maximum filtration occurs (cm s^{-1})
V – Volume of filterable seawater containing suspended particulate matter (l)
w – Descriptor related to the full width at half-maximum of a Gaussian distribution (cm s^{-1})
y_{int} – Y-intercept of linear regression relating projected area in flow to projected area in still water

particles are a mixture of organic and inorganic particulates that range in size from viruses (<0.2 µm) to larger plankters and detritus (>500 µm). Here we were able to present the ascidian with cultured phytoplankton ranging in diameter from 1 to 30 µm in a small laboratory flume to test the effects of flow speed, body size, and particle diameter.

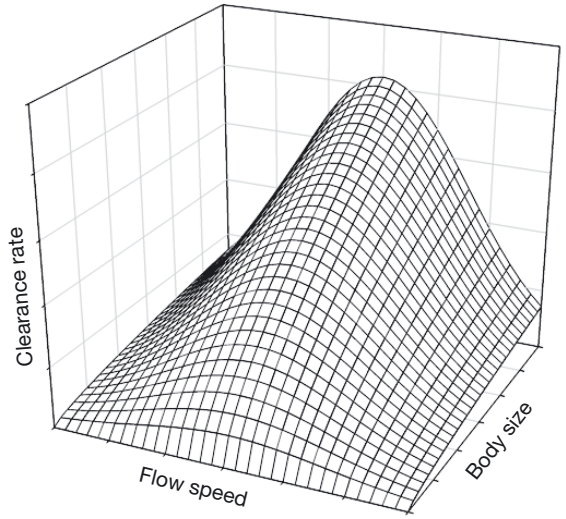

Fig. 1. Hypothesized dependence of clearance rate on flow speed and body size as described by Eq. (3). This is a generalized response surface showing both the unimodal relationship between clearance rate and flow speed, as well as the allometric response of clearance rate to body size. The specific shape of the response surface (e.g. location of maximum clearance rate) will vary with species and other factors

MATERIALS AND METHODS

Collection

Individual specimens of *Styela plicata* were collected from floating docks in the Atlantic Intracoastal Waterway near Wrightsville Beach, North Carolina, USA (34° 12′ 31″ N, 77° 47′ 47″ W). Individual ascidians were removed from the dock using a putty knife, measured, and placed in plastic bags of ambient seawater for transport to the laboratory (~15 min). Specimens were sorted in the field into 3 body size categories according to maximum contracted body length (small: <3.5 cm, intermediate: 3.5 to 4.5 cm, large: 4.5 to 6 cm). Maximum size of a specimen with siphons extended was 6.6 cm. Once in the laboratory, each ascidian was cleaned to remove epibionts, blotted dry, and attached at the base to a 6 cm long × 8 cm wide × 0.2 cm thick acrylic slide using cyanoacrylate glue. Mounting on slides facilitated immediate transferring and affixing of ascidians into the flume for experimental use.

Flume

Clearance rates were measured for varying sized specimens of *Styela plicata* in a 16.4 l, 'racetrack' flume at varying flow speeds. The flume consists of 2 parallel straight sections connected at their ends by semi-circular channels. The flume channel was 10 cm wide at all points, and water depth was maintained at 10 cm. Unidirectional water flow was created by a paddle-wheel in one of the straight sections that was connected to a gear motor (Dayton Model 2H577A) driven by a microprocessor-based controller (Dart Micro-drive II). Nominal flow speeds of 3, 14, and 22 cm s^{-1} were created and measured using an acoustic Doppler velocimeter (SonTek 16-MHz MicroADV), with the probe mounted in the center of the flume and the sample volume located 5 cm above the flume bottom (Finelli et al. 1999). For a more detailed description of the flume see Robinson et al. (2007) and Clarke et al. (2009).

Experimental protocol

Prior to the beginning of each experimental trial, the flume was filled to a depth of 10 cm (16 l) with aerated, particle-free artificial seawater (Crystal Sea) at a salinity of 35‰. A freshly collected ascidian (mounted on an acrylic slide) was transferred to the flume, where the slide was secured to the bottom such that neither siphon was pointed directly into or away from the mainstream flow. The inhalant siphon was oriented vertically such that the opening was parallel to the water surface, and the exhalant siphon was oriented horizontally with the opening normal to the water surface. Orientation of the ascidian in this manner allowed standardization across trials and was considered neutral with respect to pressure gradients driving the feeding current. The ascidian was allowed to acclimate to flow without feeding for at least 12 h. A total of 45 trials were conducted (3 body size categories × 3 flow speeds × 5 replicates).

After acclimation, 3 g of cultured and preserved algal paste consisting of diatoms and naked flagellates (Innovative Aquaculture Products, LTD) was resuspended in 400 ml of particle-free seawater and added to the flume. Three replicate 180 ml water samples were obtained by syringe from the flume at 0 and 4 h after the addition of the algal paste. Chlorophyll analysis, using a Turner Trilogy Fluorometer and following the methods of Welschmeyer (1994), confirmed that the concentration of chlorophyll *a* (chl *a*) remained above 12 µg l^{-1} during an entire feeding period, suggesting that algal concentrations were similar to those in local estuaries inhabited by *Styela plicata* (Dafner et al. 2007) and that ascidians did not become food limited during the experiment (Petersen 2007). Particle diameter distribution was measured for each sample using a laser diffraction particle size analyzer (Sequoia Scientific, LISST-Portable). The LISST analyzer provides a volumetric concentration of suspended particles (µl l^{-1}) ranging in size from 1.25 to 250 µm. Because particle volume scales as the cube of particle radius, small quantities (a few per milliliter) of particles with relatively large radii may be disproportionately represented in volumetric concentration estimates, thereby leading to spurious data. Therefore, the mid-point of each size bin was used as an estimate of the particle diameter, and assuming particles are spherical, the standard particle volume for each bin was estimated, and volumetric concentrations were converted to absolute particle concentration (particles ml^{-1}) by dividing the volume concentration by the standard particle volume. Bins with <10 particles ml^{-1} were discarded. Because the size distribution of cells within the commercial phytoplankton suspension and our manner of measuring and adding the phytoplankton to the flume were consistent, this procedure of culling bins with low concentrations of suspended particles eliminated the 12 largest particle size bins with mid-points larger than about 32 µm diameter, leaving 20 particle size bins for analysis (Fig. 2). Water samples were returned to the flume after analysis to maintain constant flume volume.

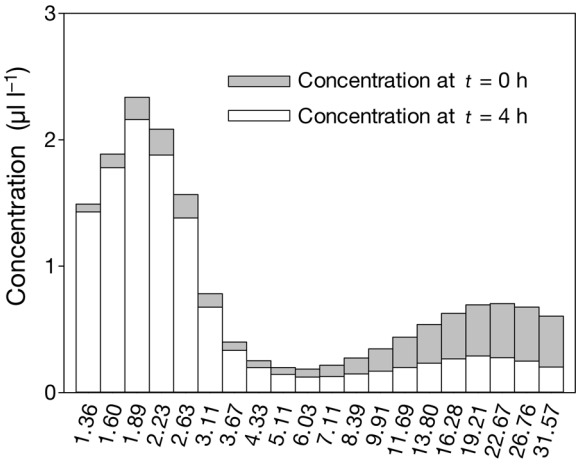

Fig. 2. Volumetric (µl l^{-1}) concentration of particles in 20 logarithmically distributed size categories at the start (time t = 0 h) and end (t = 4 h) of a feeding experiment

Body size measurements

To estimate allometric scaling of clearance rates, we measured the projected body area of ascidians in still water and flowing water, as well as their ash-free dry mass (AFDM). To measure projected body area in still water, specimens were initially placed in the flume with siphons parallel to the flume wall (90° from the 'standard' position used during feeding). Once ascidians extended their siphons, each was photographed with a digital camera and its projected body area was measured with commonly available image analysis software (ImageJ, Vers. 1.4.3.67). The ascidian was subsequently moved into a final position for feeding, and the flume was started immediately after the photograph was taken. Because ascidians bend in moving water, especially at high flow speeds, their projected body area varies with flow. It was impossible, however, to image the frontal area of ascidians in flow given the physical dimensions of the flume. Therefore, at the completion of each trial we measured the height of the ascidian above the flume bottom, then used the ratio of height in flow to the height in still water to scale the still water digital image (also with ImageJ) to estimate projected body area in flowing water. After experimental use, each ascidian was dried in an oven at 60°C for 24 h, then combusted in a muffle furnace (550°C for 3 h) to determine AFDM) (range 0.15 and 1.05 g).

Clearance rate measurements

Clearance rates (*CR*) were estimated for each ascidian at each particle size using the method outlined by Coughlan (1969):

$$CR = \frac{V}{t}\left(\ln\frac{C_{B0}}{C_{Bt}} - \ln\frac{C_{C0}}{C_{Ct}}\right) = \frac{V}{t}\ln\frac{C_{B0}C_{Ct}}{C_{Bt}C_{C0}} \quad (4)$$

where CR is clearance rate (l h^{-1}) and V is the volume of the flume. C_{Ct} is the concentration of suspended particles at time t (t = 4 h for our experiment) during a control trial, and C_{C0} is the initial concentration of suspended particles during a control trial accounting for removal of particles by gravitational deposition (Coughlan 1969, Fries & Trowbridge 2003). Similarly, C_{Bt} is the concentration of suspended particles at time t during an experimental feeding trial and C_{B0} is the initial concentration of suspended particles during a feeding trial accounting for removal of particles by deposition and feeding (Coughlan 1969, Peters 1984). Estimates of particle concentration during control trials (C_{C0}, C_{Ct}) were derived from trials using wax models of ascidians but otherwise identical to the feeding trials. Three wax models (Boekel Tackiwax) corresponding to our 3 body size categories (small, intermediate, large) were sculpted by hand, with reference to living specimens in the laboratory, to match the size and shape of a feeding ascidian. Three replicate control trials were run for each body size category at each of our nominal flow speeds (n = 27 total). The results from the 3 replicates at each body size and flow speed were averaged, and the mean particle concentration at each time period was used in the calculation of *CR* for live ascidians at the same flow speed and nearest body size. Because we used a difference procedure to estimate clearance rates, it was possible to obtain slightly negative estimates at low values of *CR*; therefore, we replaced negative values of *CR* with 0 (n = 4 instances). In all cases, *CR* was estimated using the volume concentration of suspended particles (µl l^{-1}) of suspended particles as measured by the LISST instrument; however, identical results are obtained using estimated absolute concentrations of suspended particles (particles ml^{-1}).

The clearance rate methodology relies on the use of a well-mixed test chamber. We chose a small flume (16.4 l) to ensure sufficient mixing while providing sufficient width and depth to accommodate a wide range of ascidians. Because of the small flume size, and the configuration of the paddlewheel that spans the entire cross-section, there was no opportunity of vertical or horizontal stratification. Moreover, the time scale of the experiment (4 h) is much greater than the mixing time of the flume. For example, at 3 cm s^{-1} a full transit of the flume is <1 min (<0.5% of the experimental duration). Finally, extraction of the 180 ml sample, which lasted 1 to 2 min, was performed to integrate over 1 or more transits of the flume, thus minimizing sampling bias.

Surface fitting

To fit estimated clearance rates to our model (Eq. 3), particle concentrations across all size bins were pooled to derive a total concentration of suspended particles at the beginning and end of each trial. The total clearance rate (CR_T) was then estimated using the method described above (Eq. 4). CR_T for each ascidian was then plotted against flow speed and body size, and data were fit to Eq. (3) using least-squares regression (Systat SigmaPlot v. 12).

The concentration distribution of particles in the flume exhibited 2 distinct peaks near 2 µm in diameter and near 22 µm in diameter (Fig. 2), and the

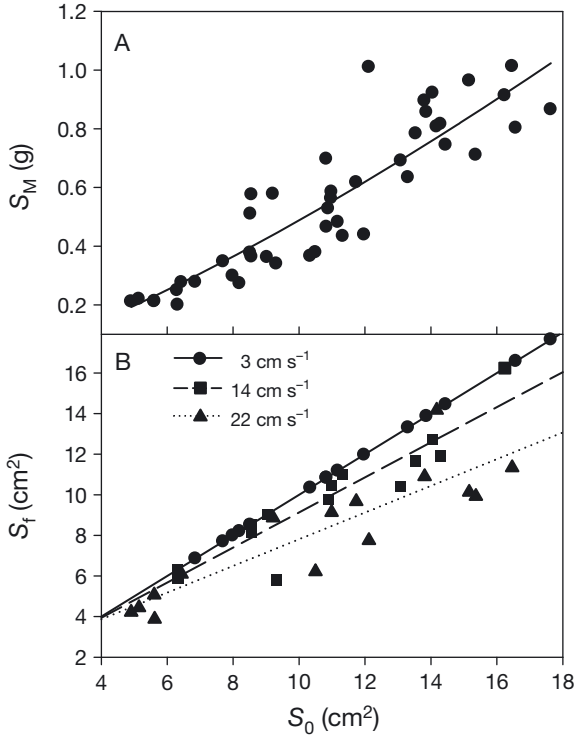

Fig. 3. (A) Power–law relationship between ash-free dry mass (S_M) and projected body area in still water (S_0). (B) Relationship between projected body area in flowing water (S_f) and projected body area in still water (S_0) showing the size- and flow-dependent alteration in the posture of ascidians in our flume experiment. Regression results and coefficients for both analyses are listed in Table 1

relationship between *CR* and particle diameter changed slope at a point near 10 µm. Therefore, to estimate the influence of particle diameter on *CR*, the 20 particle size bins were arbitrarily grouped into 2 categories such that the 13 particle size bins with diameters <10 µm were considered the 'small' particle group and the 7 particle size bins with diameters >10 µm were considered the 'large' particle group. Using these groupings, clearance rates of small particles (CR_S) and large particles (CR_L) were estimated as well. These estimates were similarly plotted and fit to Eq. (3) using least-squares regression (Systat SigmaPlot v. 12).

RESULTS

Ascidian body size

Because the term body size is used with variable meaning in the literature on suspension feeding, we estimated ascidian body size using 3 related measures: ash-free dry mass (S_M), projected body area in still water (S_0), and projected body area in flow (S_f). There was a strong power–law relationship between S_M and S_0 (Fig. 3A, Table 1A). The relationship between S_0 and S_f, however, is more complex, with the additional influence of flow speed (Fig. 3B). We initially fit S_f to both S_0 and U using a least-squares planar regression with the result S_f = 2.69 (±0.66 SE) + 0.82 (±0.05 SE)S_0 − 0.14 (±0.02 SE) U (R^2 = 0.88, n = 45, p < 0.01). However, for clarity in presentation and to highlight the flow-dependent change in body posture, we grouped the ascidians by nominal flow treatment (3, 14, and 22 cm s^{-1}) and analyzed the relationship between S_0 and S_f using separate linear regressions (Fig. 3B, Table 1B). At 3 cm s^{-1} there was no change in body orientation, such that the slope of the regression was 1 (Fig. 3B, Table 1B). However, as flow speed increased, the ascidians increasingly bent so that the slopes of the regressions decreased to 0.86 in 14 cm s^{-1} flow (Table 1B) and to 0.66 in 22 cm s^{-1} flow (Fig. 3B, Table 1B).

Table 1. Results and regression coefficients (±SE) for analyses of the relationship between the body size metrics depicted in Fig. 3. (A) Ash-free dry mass (S_M) vs. projected area in still water (S_0); $S_M = s_s S_0^{bs}$, (B) Projected area in flow (S_f) vs. projected area in still water (S_0); $S_f = mS_0 + y_{int}$. Other constants and variables defined in Box 1

(A) S_M vs. S_0				
s_s	b_s	R^2	p	n
0.024 (±0.007)	1.30 (±0.11)	0.81	<0.001	45
(B) S_f vs. S_0				
U	m	y_{int}	R^2	p	n
3	1 (±0.00)	0 (±0.00)	1.00	<0.001	15
14	0.86 (±0.1)	0.49 (±1.1)	0.85	<0.001	15
22	0.66 (±0.1)	1.23 (±1.1)	0.78	<0.001	15

Clearance rates

Particle-size-dependent *CR* (Fig. 4) showed consistent variation with both body size and flow speed. For all body size categories, *CR* varied asymptotically or unimodally with particle diameter depending on flow speed. At all flow speeds, *CR* increased directly as particle diameter increased to ~10 µm (Fig. 4). The response of *CR* as particle diameter increased beyond 10 µm was flow dependent. At 3 and 22 cm s^{-1}, *CR* approached an asymptote at the peak value (Fig. 4A,C). In contrast, at 14 cm s^{-1}, *CR* declined steadily as particle diameter increased above 10 µm.

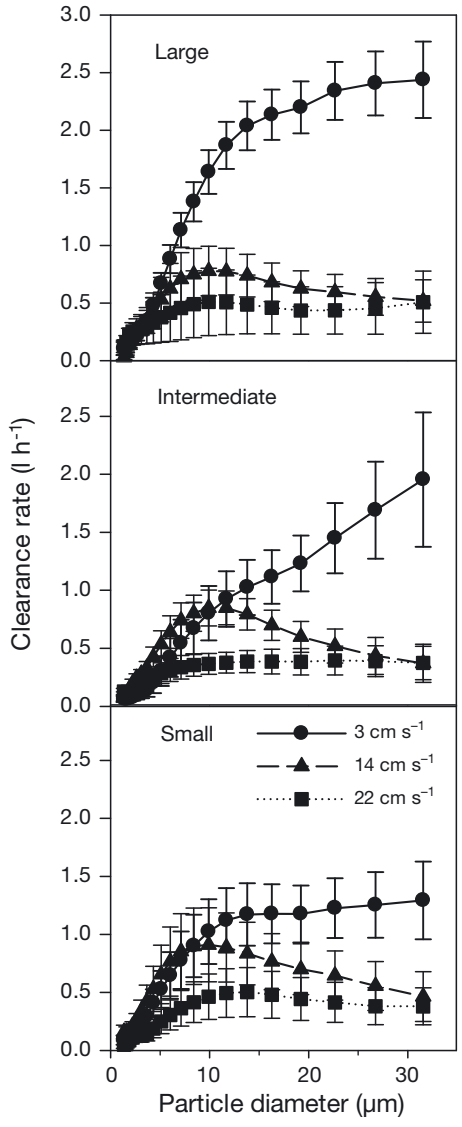

Fig. 4. Estimated clearance rates for (A) large (4.5 to 6.5 cm), (B) intermediate (3.5 to 4.5 cm), and (C) small (<3.5 cm) ascidians as a function of particle size and flow speed. Error bars represent standard errors of the mean of 5 replicates

Moreover, maximal *CR* decreased with increasing flow speed such that the maximum *CR* at 3 cm s^{-1} was generally greater than the maximum *CR* at 14 or 22 cm s^{-1} (Fig. 4). Body size category had a more pronounced effect on *CR* at 3 cm s^{-1} than at the faster flows (Fig. 4). For example, at 3 cm s^{-1} large ascidians cleared the water at a rate that was 2 to 3 times that of intermediate and small ascidians. The effect of body size was much smaller at faster flow speeds (Fig. 4).

The trends observed in the analyses of *CR* for individual particle size bins are reflected in the surface plots of *CR* vs. AFDM and flow speed. Maximum CR_S (Fig. 5A) and CR_T (Fig. 5C) were 5 to 10 times lower than CR_L (Fig. 5B). Fitting CR_S and CR_T to Eq. (3) resulted in surface fits with $R^2 < 0.3$ (Table 2). These fits are consistent with the lower absolute *CR* estimates that do not vary much with body size or with flow speed. More robust fits ($R^2 > 0.5$) were generated CR_L, which tended to be more sensitive to both body size and flow speed. The overall regressions for all fits were statistically significant ($p \leq 0.05$), with the exception of CR_S fitted against projected body area in flowing water for which $p = 0.06$ (Table 2).

The relationship between *CR* within each particle size class and body size or flow speed was remarkably consistent regardless of how body size was defined (Table 2). In general, the allometric exponent, *b*, was lower for CR_S and CR_T than for CR_L (Table 2). This reflects the sensitivity of CR_L to body size. Values of *b* were also lower for the relationship between *CR* and S_M than for the relationship between *CR* and projected body area in still water (S_0) or projected body area in flow (S_f) (Table 2). This suggests that clearance was more sensitive to changes in projected body area (in still water and in flowing water) than to changes in body mass; a phenomenon that is mathematically consistent with the relationship between AFDM and projected body area in still water ($S_M = 0.024\ S_0^{1.30}$; Fig. 3A). Because we found similar patterns when relating clearance rates to our 3 body size metrics (Table 2), we present all subsequent results in terms of S_M, as this variable is used frequently in the literature on suspension feeding.

The relationship between clearance rate and flow speed was more complex than the allometric relationships. CR_S (Fig. 5A) and CR_T (Fig. 5C) exhibited the expected unimodal response to flow speed, with peaks near 12 and 8 cm s^{-1}, respectively (Table 2). In contrast, CR_L showed steady declines with increasing flow speed, with the peak *CR* occurring near 0 cm s^{-1} (Fig. 5B). Fitting other forms of unimodal distributions, including those with asymmetrical peaks, indicated that the simple symmetrical peak used here provided the best overall fit to our data. For example, a modified log-normal response of clearance rate to increasing flow speed resulted in only a slight improvement of fit to CR_L but a slightly worse fit to CR_S and CR_T.

DISCUSSION

Feeding by benthic suspension feeders is a critical ecological process that is sensitive to a number of intrinsic and extrinsic factors. We have presented the results of a flume experiment testing the interactive

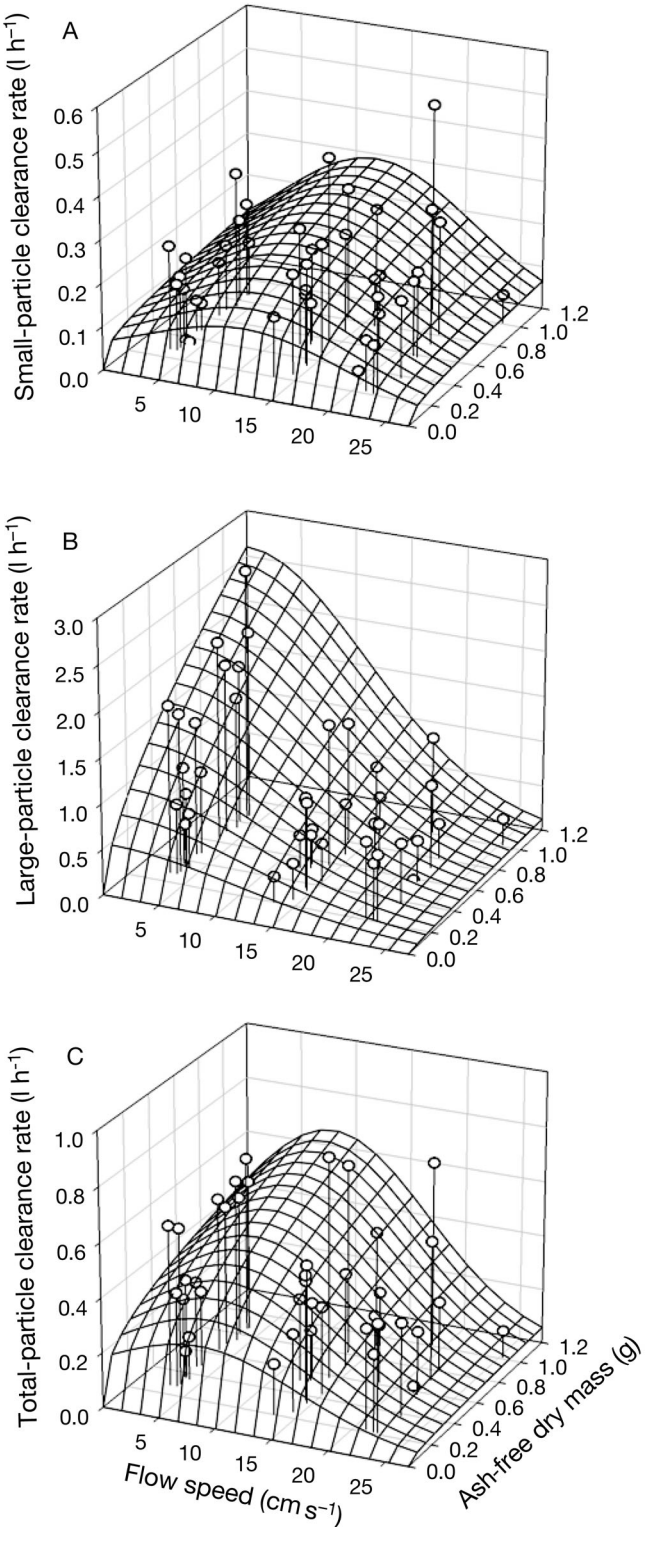

Fig. 5. Response of (A) small-particle, (B) large-particle, and (C) total-particle clearance rates to flow speed and ash-free dry mass (S_M). The surface represents the best fit for Eq. (3). Parameters as described in Table 2

effects of body size and flow speed on particle-size-dependent clearance rates of the ascidian *Styela plicata*. Our results indicate consistent allometric scaling of clearance rates with body size measured as both projected body area and body mass, and a strong influence of flow speed on clearance rates that depends on particle diameter.

Clearance response to increasing body size

Dimensional analysis of the planar area of feeding structures and body volume suggests that feeding rate of suspension feeders should scale as body mass raised to the two-thirds power (i.e. $b = 0.67$; Klumpp 1984, Schmidt-Nielsen 1997). Our results suggest that CR_L by *Styela plicata* scales roughly according to this two-thirds power law (Table 2, Fig. 5B), while CR_S and total particles was less affected by variation in AFDM ($b < 0.67$; Table 2, Fig. 5A,C). We derived slightly higher estimates of b when relating clearance rate to projected body area (S_0, S_f) rather than AFDM (S_M). This result is mathematically consistent with the non-linear relationship we found between AFDM (S_M) and projected S_0. For example, we found that $CR_L \propto S_M^{0.62}$. Substituting $S_M = 0.024 S_0^{1.30}$ yields $CR_L = (S_0^{1.30})^{0.62} = S_0^{0.81}$, which is slightly greater than the value of $b = 0.76$ found through our regression analysis (Table 2). Given the strong relationship between our 3 metrics of body size, it is not surprising that the overall trends for clearance rates were consistent between S_M, S_0, and S_f.

Our estimates of b are similar to or lower than others reported in the literature (Table 3). While the majority of literature reports estimate b to be near 0.67, differences among species and experimental methods have resulted in a wide range of reported estimates (Randløv & Riisgård 1979, Klumpp 1984). A number of other factors have been invoked to explain this wide range. Holmes (1973), for example, attributed small allometric exponents for *Ascidiella aspersa* to animal disturbance. Interestingly, he also found higher estimates of b in flowing water, which may be an indication of increased clearance due to increased particle flux. Allometric exponents in Table 2 approximately equal to 1 are surprising and considered to be due to a lack of low-mass specimens (Klumpp 1984) or due to non-isometric growth of the tunic compared with total mass (Randløv & Riisgård 1979).

Our data suggest that the relatively low estimates of b for CR_S and CR_T result, at least in part, from the interaction of body size and flow speed. For example,

Table 2. Results and regression coefficients (±SE) for analysis of clearance rates as a function of flow speed and body size, as depicted in Fig. 5 (n = 45). The overall p-value is associated with the planar regression fitting data to Eq. (3). Constants and variables defined in Box 1

Body size metric	R^2	p	s_c (l h^{-1})	b	U_p (cm s^{-1})	w (cm s^{-1})
Ash-free dry mass (S_M)						
CR_S	0.174	0.048	0.27 ± 0.05	0.28 ± 0.23	11.9 ± 1.3	8.7 ± 1.8
CR_L	0.549	<0.001	2.32 ± 0.73	0.62 ± 0.20	0.0 ± 10.9	10.9 ± 6.0
CR_T	0.278	0.004	0.61 ± 0.13	0.33 ± 0.23	8.0 ± 1.7	8.6 ± 2.3
Projected body area in still water (S_0)						
CR_S	0.172	0.050	0.09 ± 0.07	0.41 ± 0.34	12.2 ± 1.3	8.8 ± 1.8
CR_L	0.527	<0.001	0.24 ± 0.19	0.76 ± 0.29	0.0 ± 12.0	11.5 ± 6.8
CR_T	0.273	0.004	0.16 ± 0.14	0.46 ± 0.35	8.3 ± 1.6	8.7 ± 2.4
Projected body area in flow (S_f)						
CR_S	0.162	0.06	0.11 ± 0.08	0.33 ± 0.34	12.5 ± 1.5	9.0 ± 1.9
CR_L	0.516	<0.001	0.27 ± 0.21	0.71 ± 0.29	0.0 ± 13.5	12.0 ± 8.1
CR_T	0.260	0.006	0.22 ± 0.18	0.35 ± 0.35	8.4 ± 1.7	8.9 ± 2.6

Table 3. Literature estimates of the allometric scaling constants (s_c) and exponents (b) relating clearance rate to body mass

Species	Body mass (g)	Food-particle diameter range (µm)	s_c (l h^{-1})	b	Flow	Source
Pyura stolonifera	0.1–19[a]	6–50	0.49–0.94	0.7–1.08	Stirred at unknown rate	Klumpp (1984)
Ciona intestinalis	0.05–0.18[a]	4.8–8	7.08	0.68	Static	Petersen & Riisgård (1992)
Ciona intestinalis	0.03–0.4[a]	1–7	2.78	0.84	Stirred at unknown rate	Randløv & Riisgård (1979)
Ascidiella aspersa	0.04–0.8[a]	1–7	3.26	1.05		
Ascidiella aspersa	0.1–1.0[a]	8–12	0.96–3.18	0.275–0.607	Static & flow through at unknown rate	Holmes (1973)
Styela clava	0.1–1.0[a]	8–12	0.52–5.76	0.415–0.646		
Styela plicata	1.2–1.9[a]	7–8	0.44[c]	0.934[c]	Static	Fiala-Médioni (1978)
Styela plicata	0.15–1.05[b]	1.25–10	0.27	0.28	Unidirectional, flume (3–22 cm s^{-1})	Present study
		10–32	2.32	0.62		
		1.25–32	0.61	0.33		

[a]Dry mass; [b]ash-free dry mass; [c]calculated by the authors from published data values

when the confounding influence of flow speed was removed by calculating b for S_M in the slow-flow treatments only, estimates of b increased to 0.46 for CR_S, 0.75 for CR_L, and 0.54 for CR_T. These values are much closer to the expected 0.67, indicating that flow speed has a strong influence on the allometric response of clearance rate to body size by disproportionately depressing feeding of larger ascidians. This result is also evident in the shape of the curves shown in Fig. 4; the effect of flow speed on clearance rate is much more pronounced for large ascidians than for intermediate and small ascidians. We also note that CR_L, for which b was consistently closest to 0.67, was highest in our low-flow treatment across body sizes, again indicating a strong interaction of body size, flow speed, and particle size.

The interactive effect of body size and flow speed on clearance rates may arise from 2 sources. First, exposure of *Styela plicata* to flow resulted in a predictable change in body posture, as the ascidian had a tendency to 'lay-over' as flow increased (Fig. 3B). Presumably, because active suspension feeders generate their own feeding currents and their feeding structures are often internal, feeding should be relatively insensitive to changes in posture. Nevertheless, it is reasonable that a change in body posture may influence clearance rates by positioning siphons closer to the substratum where speeds are slower (Sponaugle & LaBarbera 1991), by orienting the siphons so that the animal benefits from passive flow (Young & Braithwaite 1980, Knott et al. 2004), or when bending compresses the pharynx or otherwise

disrupts pumping. Second, the interaction between body size and flow speed may be related to the ability of the ascidian to entrain particles into their feeding current (e.g. Okamura 1987). The strength of the ascidian pump scales with body size, so that larger individuals generate a stronger feeding current and may be better able to deflect particles into their feeding stream. For example, such a mechanism may explain why larger ascidians have a higher clearance rate than smaller ascidians at 3 cm s^{-1}; these large animals, by virtue of their stronger pump, are able to access more of the water column. This mechanism is further supported by our finding that clearance of larger particles, which carry more momentum and are more likely to resist deflection into the feeding current, were highest in slow flow and were more affected by flow speed than small particles (Fig. 4).

Clearance response to increasing flow speed

The response of *CR* to flow speed was particle size dependent (Figs. 4 & 5), suggesting an interaction between particle diameter, flow speed, and particle capture dynamics. CR_S exhibited a unimodal response to increasing flow speed with a peak near 12 cm s^{-1} that declined 3-fold as flow increased to 22 cm s^{-1} or decreased to 3 cm s^{-1}. In contrast, CR_L exhibited a steady decline with increasing flow speed, with a peak near 0 cm s^{-1} that declined nearly 10-fold as flow speed increased to 22 cm s^{-1}. The relative insensitivity of CR_S and increased sensitivity of CR_L to flow speed suggests that *Styela plicata* had a more difficult time capturing large particles in high flows. This progressive loss of ability to entrain or capture large particles with increasing flow speeds may be attributed to the proportionately greater momentum carried by these particles (Okamura 1987).

Previous studies have shown that ascidians trap particles with high efficiency. Randløv & Riisgård (1979) demonstrated that retention efficiency of 4 species approached 100% for particles 3 to 6 µm in diameter. Similarly, Fiala-Médioni (1978) and Klumpp (1984) found average retention efficiencies of 65 to 100% for particles up to 50 µm. Our approach indicates that clearance rates measured under flume flows may not always reflect these high retention rates. We suggest that the interaction of water flow with particle delivery (i.e. entrainment into the feeding current) and body posture creates conditions that are not optimal for feeding. Importantly, most earlier studies were conducted under ideal conditions of small chamber volume and minimal flow that favored maximal feeding rates and would be unable to capture the dynamics that we report. Rather than being contradictory, these 2 approaches represent feeding under varying conditions and likely capture important aspects of the field situation.

Few studies have investigated the response of clearance rate to increasing flow speed; however, growth rate is often used as a proxy for feeding rates, especially for bivalves. Many such studies have indicated a unimodal or declining response of growth rate with increasing flow speed. For example, Kirby-Smith (1972), Cahalan et al. (1989), and Eckman et al. (1989) independently found that growth rates of the bay scallop *Argopectin irradians* decline with increasing flow speed. The growth rate of the giant scallop *Placopecten magellanicus* was found to increase steadily between flow speeds of 0 and 5 cm s^{-1}, after which it declined with speeds up to 18 cm s^{-1} (Wildish et al. 1987). Additionally, decreased clearance rates of *P. magellanicus* support the hypothesis that reduced growth is due to inhibited filtration (Wildish et al. 1992, Wildish & Saulnier 1993). A similar reduction in growth due to enhanced flow may also be true of *Styela plicata*, as we noted that the size distribution of *S. plicata* at the collection site was inversely proportional to flow speed such that the smallest animals were found in the highest flows.

The interaction between flow speed and particle diameter in determining the clearance rates of *Styela plicata* may have important implications. For example, in this study, *S. plicata* was able to maintain a relatively constant level of feeding on small diameter particles across a range of flow speeds. In contrast, clearance rates of large particles were greater in magnitude, but declined more rapidly with flow speed. If these results extend to field conditions, they may indicate spatial or temporal (e.g. tidal) shifts in diet and material processing. For example, *S. plicata* may preferentially feed on large phytoplankton at slack tides, whereas feeding on small phytoplankton or bacteria may be relatively constant throughout the tidal cycle.

While we have placed our results in the context of particle-size-dependent feeding, it is also possible that the difference in particle removal from the flume exhibited between large and small particles is due to the type of phytoplankton in each size class. The algal suspension used here was a mixture of naked flagellates and diatoms that likely corresponded, respectively, to the 2 size peaks noted in Fig. 2. These 2 types of phytoplankton likely differ in both biochemical and physical properties such that differen-

tial removal from suspension may result from active rejection by the ascidian or physical processes associated with active suspension feeding. Ascidians are known to reject large particles (>100 µm) at the siphon (Robbins 1984, Petersen 2007), such that these particles never enter the branchial basket and remain in suspension. However, there is no evidence of this type of active selection within the particle size range used here. If active discrimination of particles was occurring, it was likely occurring at the mouth. Any particles rejected at this stage would be bound in mucus and expelled as pseudofeces, and their removal from suspension would be indistinguishable from feeding. As such, because we observed differential removal of particles from suspension, it is most likely that the sorting process coincided with entrainment of the particles into the feeding current. Differences at this stage are likely due to the physical properties of the cell, such as density, that influence particle inertia.

The importance of these findings is compounded by considering that the carbon and energy content of the phytoplankton cells generally scales with cell volume (Mullin et al. 1966, Strathmann 1967, Putt & Stoeker 1989, Verity et al.1992). Verity et al. (1992) found that nanoplankton (cell diameter < 20 µm) are more carbon dense than larger phytoplankton, suggesting the relationship between carbon content and cell volume is non-linear. For example, using conversions found in Verity et al. (1992), the organic carbon content of a cell with a diameter of 2.5 µm is ~3 pg (cell volume 8.2 $\mu m^3 \times 0.36$ pg μm^{-3}), while a cell with a diameter of 25 µm has an organic carbon content of ~1310 pg (= 8181 $\mu m^3 \times 0.16$ pg μm^{-3}). The larger cell has ~443-fold as much carbon as the smaller cell, rather than 1000-fold as much. It follows, then, that feeding on smaller particles may be more efficient with respect to the amount of carbon ingested per cell. The benefits of targeting smaller particles to the feeding organism will depend on the energetic cost of removing particles of a given size from suspension. If our results showing a steep decline in CR_L with increasing flow speed (Fig. 5B) are derived from increased momentum in larger particles, we may assume that capture of large particles requires greater energetic input (i.e. greater pumping effort). Thus, continual feeding on abundant but small particles supplemented with larger particles during periods of slow flow (i.e. easier capture) may make good energetic sense. Such hypotheses should be examined by directly testing whether feeding is related to particle inertia and the energetic cost of particle capture.

We have shown that feeding in a cosmopolitan tunicate species is modulated by the interaction of body size, particle diameter, and flow speed. The most striking result is the contrast between the nearly constant clearance of small particles versus the more variable clearance of large particles. This flow-dependent shift in clearance of different size particles is potentially important for understanding patterns of material processing in a variety of contexts. Most notably, removal of bacteria and small-phytoplankton-sized particles by *Styela plicata* seems to occur across a wide range of flow speeds, while removal of larger phytoplankton occurs primarily at slower flows. Such flow-mediated feeding may influence the strength and dynamics of benthic–pelagic coupling or when and how benthic suspension feeders can be used in bioremediation. Moreover, this type of information may be used in the design of mariculture facilities to provide a competitive advantage to commercially important species over fouling organisms, such as *S. plicata*.

Acknowledgements. This research was funded in part by grants OCE-0751753, OCE-0715271, and OCE-0715272 from the National Science Foundation to C.M.F., the UNCW Marine Science Program and the UNCW Department of Biology and Marine Biology. Dr. M. Posey, Dr. L. Leonard, and the members of the Marine Biofluiddynamics and Ecology Laboratory provided thoughtful comments on previous versions of this manuscript. We are also grateful for the field assistance of Tse-Lynn Loh and Lou Muzyczek.

LITERATURE CITED

Cahalan JA, Siddall SE, Luckenbach MW (1989) Effects of flow velocity, food concentration and particle flux on growth rates of juvenile bay scallops, *Argopecten irradians*. J Exp Mar Biol Ecol 129:45–60

Clarke RD, Finelli CM, Buskey EJ (2009) Water flow controls the distribution and feeding behavior of two co-occurring coral reef fishes. II. Laboratory measurements. Coral Reefs 28:475–488

Cloern JE (1982) Does the benthos control phytoplankton biomass in South San Francisco Bay? Mar Ecol Prog Ser 9:191–202

Coughlan J (1969) The estimation of filtering rate from the clearance of suspensions. Mar Biol 2:356–358

Dafner EV, Mallin MA, Souza JJ, Wells HA, Parsons DC (2007) Nitrogen and phosphorous species in the coastal and shelf waters of southeastern North Carolina, mid-Atlantic U.S. Coast. Mar Chem 103:289–303

Eckman J, Peterson C, Cahalan J (1989) Effects of flow speed, turbulence and orientation on growth of juvenile bay scallops, *Argopecten irradians concentricus*. J Exp Mar Biol Ecol 132:123–140

Fiala-Médioni A (1978) Filter-feeding ethology of benthic invertebrates (ascidians). IV. Pumping rate, clearance rate, filtration efficiency. Mar Biol 48:243–249

Finelli CM, Hart DD, Fonseca DM (1999) Evaluating the spatial resolution of an acoustic Doppler velocimeter and the consequences for measuring near-bed flows. Limnol Oceanogr 44:1793–1801

Finelli CM, Hart DD, Merz RA (2002) Stream insects as passive suspension feeders: the effects of velocity and food concentration on feeding performance. Oecologia 131: 145–153

Fries JS, Trowbridge JH (2003) Flume observations of enhanced fine-particle deposition to permeable sediment beds. Limnol Oceanogr 48:802–812

Holmes N (1973) Water transport in the ascidians *Styela clava* Herdman and *Ascidiella aspersa* (Müller). J Exp Mar Biol Ecol 11:1–13

Jorgensen CB (1966) Biology of suspension feeding. Pergamon Press, Oxford

Kirby-Smith WW (1972) Growth of the bay scallop: the influence of experimental water currents. J Exp Mar Biol Ecol 8:7–18

Klumpp DW (1984) Nutritional ecology of the ascidian *Pyura stolonifera*: influence of body size, food quantity and quality on filter-feeding, respiration, assimilation efficiency and energy balance. Mar Ecol Prog Ser 19: 269–284

Knott NA, Davis AR, Buttemer WA (2004) Passive flow through an unstalked intertidal ascidian: orientation and morphology enhance suspension feeding in *Pyura stolonifera.* Biol Bull 207:217–224

Mullin MM, Sloan PR, Eppley RW (1966) Relationship between carbon content, cell volume, and area in phytoplankton. Limnol Oceanogr 11:307–311

Officer CB, Smayda TJ, Mann R (1982) Benthic filter feeding: a natural eutrophication control. Mar Ecol Prog Ser 9:203–210

Okamura B (1987) Particle size and flow velocity induce an inferred switch in bryozoan suspension-feeding behavior. Biol Bull 173:222–229

Peters RH (1984) Methods for the study of feeding, grazing and assimilation by zooplankton. In: Downing JA, Rigler FH (eds) A manual on methods for the assessment of secondary productivity in fresh waters, 2nd edn. IBP Handbook 17. Blackwell Scientific, Oxford, p 336–412

Petersen J (2007) Ascidian suspension feeding. J Exp Mar Biol Ecol 342:127–137

Petersen J, Riisgård HU (1992) Filtration capacity of the ascidian *Ciona intestinalis* and its grazing impact in a shallow fjord. Mar Ecol Prog Ser 88:9–17

Putt M, Stoeker DK (1989) An experimentally determined carbon:volume ratio for marine oligotrichous ciliates from estuarine and coastal waters. Limnol Oceanogr 34: 1097–1103

Randløv A, Riisgård HU (1979) Efficiency of particle retention and clearance rate in four species of ascidians. Mar Ecol Prog Ser 1:55–59

Robbins IJ (1984) The regulation of ingestion rate at high suspended particulate concentrations, by some phleobranchiate ascidians. J Exp Mar Biol Ecol 82:1–10

Robinson HE, Finelli CM, Buskey EJ (2007) The turbulent life of copepods: effects of water flow over a coral reef on their ability to detect and evade predators. Mar Ecol Prog Ser 349:171–181

Schmidt-Nielsen K (1997) Animal physiology: adaptation and environment, 5th edn. Cambridge University Press, New York, NY

Sherrard KM, LaBarbera M (2005) Form and function in juvenile ascidians. II. Ontogenetic scaling of volumetric flow rates. Mar Ecol Prog Ser 287:139–148

Shimeta J, Jumars P (1991) Physical mechanisms and rates of particle capture by suspension feeders. Oceanogr Mar Biol Annu Rev 29:191–257

Sponaugle S, LaBarbera M (1991) Drag-induced deformation: a functional feeding strategy in two species of gorgonians. J Exp Mar Biol Ecol 148:121–134

Strathmann RR (1967) Estimating the organic carbon content of phytoplankton from cell volume or plasma volume. Limnol Oceanogr 12:411–418

Verity PG, Robertson CY, Tronzo CR, Andrews MG, Neson JR, Sieracki ME (1992) Relationships between cell volume and the carbon and nitrogen content of marine photosynthetic nanoplankton. Limnol Oceanogr 37: 1434–1446

Welschmeyer N (1994) Fluorometric analysis of chlorophyll *a* in the presence of chlorophyll *b* and pheopigments. Limnol Oceanogr 39:1985–1992

Wildish DJ, Kristmanson DD (1997) Benthic suspension feeders and flow. Cambridge University Press, Cambridge

Wildish DJ, Saulnier AM (1993) Hydrodynamic control of filtration in the giant scallop. J Exp Mar Biol Ecol 174: 65–82

Wildish DJ, Kristmanson DD, Hoar RL, DeCoste AM, McCormick SD, White AW (1987) Giant scallop feeding and growth responses to flow. J Exp Mar Biol Ecol 113: 207–220

Wildish DJ, Kristmanson DD, Saulnier AM (1992) Interactive effect of velocity and seston concentration on giant scallop feeding inhibition. J Exp Mar Biol Ecol 155:133–143

Young CM, Braithwaite LF (1980) Orientation and current-induced flow in the stalked ascidian *Styela montereyensis.* Biol Bull 159(2):428–440

Editorial responsibility: Kenneth Heck Jr., Dauphin Island, Alabama, USA

Submitted: Januray 23, 2013; Accepted: September 20, 2013
Proofs received from author(s): December 11, 2013